Journal of Signal Processing, Vol.27, No.4, pp.129-132, July 2023

SELECTED PAPER AT NCSP'23

Attitude Control of Biped Hopping Robot Using Inertial Rotor

Ayumu Kato, Hiroshi Suzuki, Takahiro Kitajima,
Akinobu Kuwahara and Takashi Yasuno

Graduate School of Science and Technology for Innovation, Tokushima University
2-1 Minami-Josanjima, Tokushima 770-8506, Japan
E-mail: katoh-a@ee.tokushima-u.ac.jp
{suzuki.hiroshi, yasuno.takashi}@tokushima-u.ac.jp

Abstract

We propose attitude stabilization control for a biped hopping robot with springs and a closed-link leg mechanism. The robot has an inertial rotor to stabilize the attitude in combination with the swinging control of the leg. The attitude stabilization control is realized using an integral optimum servo controller designed on the basis of the linear quadratic regulator method. The attitude of the robot is estimated from the acceleration of the robot body measured by an IMU. Experiments using this system are conducted to confirm the attitude stabilization performance compared with the simulation results.

1. Introduction

Moving motions of biped-leg-type movement mechanisms have been studied to expand the field of robot use. The advantages of a leg-type movement mechanism are good adaptability to uneven and discontinuous terrain, and the ability to move over large holes and obstacles by hopping motion. However, different from wheeled, crawler, and even multi-legged robots, the biped-leg-type robot is less stable and cannot stand on its own without stabilization control. Moreover, the center of gravity of the robot changes greatly during hopping and moving motions, since the hopping motion is often accompanied by the expansion and contraction of the legs. Therefore, in order to enhance the mobility of the leg-type robot, a strong attitude stabilization capability is required.

In this paper, we propose attitude control for a biped hopping robot using an inertial rotor in order to realize hopping and moving control. The robot has an inertial rotor to stabilize the attitude combination with the swinging control of the leg. Attitude stabilization control is realized using an integral optimum servo with the linear quadratic regulator (LQR) method, which is robust to modeling errors [1]. The usefulness of the proposed system and the performance of the attitude controller have already been verified from simulation results [2]. Therefore, in this study, the effectiveness of the proposed system is investigated by implementing it to an actual robot and comparing it with simulation result.

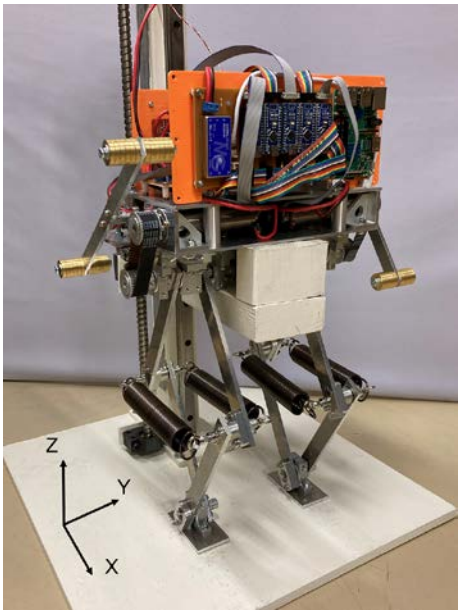

Figure 1: Appearance of developed hopping robot

2. Hopping Robot

Figure 1 shows the developed biped hopping robot with springs and closed-link legs. The robot has a mass of 7.11 kg and a height of 504 mm in the self-standing state. The springs store energy when the robot lands and release it when the robot jumps. The closed-link leg mechanism is employed to take advantage of the elastic property of the spring effectively. Moreover, the robot has an inertial rotor on its body to realize stable hopping and moving control. The moment of inertia of the rotor can be adjusted by changing the number of weights attached to the tips of inertial rotor. The legs of the robot are designed to be lightweight and have a small moment of inertia by setting actuators on the main body. Therefore, the robot has both an agile motion ability owing to a high center of gravity and a rapid leg motion during hopping.

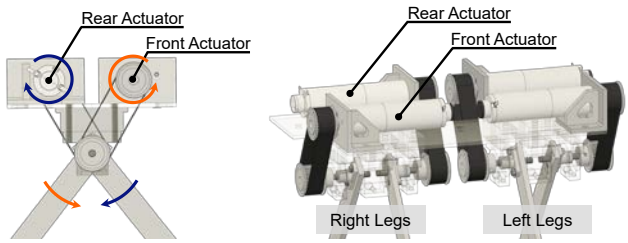

(a) Side view **(b)** 3D view

Figure 2: Closed-link legs mechanism

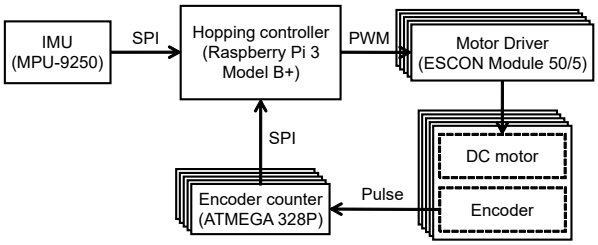

Figure 3: System configuration of hopping robot

2.1 Hardware configuration of robot

Figure 2 shows the mechanism of closed-link legs. Each leg has two degrees of freedom, i.e., extending and swinging, which are controlled by a combination of two actuators. This mechanism can use the output of the actuators efficiently since both actuators contribute to leg extension simultaneously. The leg opens and closes by driving the actuators in opposite directions, and the leg swings by driving them in the same direction. Attitude stabilization control is performed by combining the inertial rotor and swinging the legs.

Table 1 shows the specifications of the DC geared motor (maxon DXC26L GB KL 24V) used by the legs and inertial rotor. The motor has an incremental encoder to measure the revolution speed. The gear ratio of the motor for the inertial rotor is set high since the inertial rotor requires sufficient torque to obtain a reaction force for attitude stabilization. On the other hand, the gear ratios of the leg motors are set relatively low to realize a rapid leg motion since the leg extension is assisted by the springs.

Table 1: Actuator specifications

	Legs	Rotor
Nominal voltage [V]	24	24
Gear ratio	35:1	62:1
Max. continuous torque [Nm]	1.52	2.33
Max. output power [W]	32	28

2.2 System configuration

Figure 3 shows a system configuration of the hopping robot. The controller of the robot is implemented on Raspberry Pi 3 Model B+. The controller sends a desired current to the motor driver using PWM signals, since the motor's torque is controlled by using the motor driver. The encoder counter counts quadrature signals from an incremental encoder that outputs pulse in accordance with the rotation angle of the motor, and it sends the counted result to the controller by SPI communication. The IMU sensor measures three-dimensional accelerations to estimate the robot attitude even in air.

The power of the robot 24 V is supplied externally and the power supply of the control system 5 V is generated using a DC/DC converter equipped on the robot.

3. Attitude Control

The hopping motion of a biped robot is structurally unstable, and attitude stabilization control is indispensable. Therefore, the attitude controller is designed as an integral optimum servo based on the LQR method, which has a large stability margin and robustness to modeling errors. The controller is designed by linearizing the motion equation of the robot in the near-self-standing state, since the LQR is premised on applying linear systems.

The robot model is represented by the general linear system state equation

$$\dot{\boldsymbol{x}} = \boldsymbol{A}\boldsymbol{x} + \boldsymbol{B}\boldsymbol{u} \tag{1}$$

where $\boldsymbol{x} \in \mathbb{R}^n$ is the state of the system and $\boldsymbol{u} \in \mathbb{R}^m$ is the input of the system. The input of the LQR method is the optimum input that minimizes the quadratic evaluation function

$$\int_0^\infty \left(\boldsymbol{x}^{\mathrm{T}}\boldsymbol{Q}\boldsymbol{x} + \boldsymbol{u}^{\mathrm{T}}\boldsymbol{R}\boldsymbol{u}\right) dt \tag{2}$$

where $\boldsymbol{Q} \in \mathbb{R}^{n\times n}$ is the state weight matrix and $\boldsymbol{R} \in \mathbb{R}^{m\times m}$ is the input weight matrix. In the integral optimum servo, the system is extended to the deviation system, and the evaluation function is defined as

$$\int_0^\infty \left(\tilde{\boldsymbol{x}}^{\mathrm{T}}\boldsymbol{Q}_1\tilde{\boldsymbol{x}} + \tilde{\boldsymbol{w}}^{\mathrm{T}}\boldsymbol{Q}_2\tilde{\boldsymbol{w}} + \tilde{\boldsymbol{u}}^{\mathrm{T}}\boldsymbol{R}\tilde{\boldsymbol{u}}\right) dt \tag{3}$$

where $\tilde{\boldsymbol{x}} \in \mathbb{R}^n$, $\tilde{\boldsymbol{w}} \in \mathbb{R}^m$, and $\tilde{\boldsymbol{u}} \in \mathbb{R}^m$ are the state deviation, state deviation integral values, and input deviation, and $\boldsymbol{Q}_1 \in \mathbb{R}^{n\times n}$ and $\boldsymbol{Q}_2 \in \mathbb{R}^{m\times m}$ are weight matrices of the state deviation and state deviation integral values, respectively. Now, using the solution $\boldsymbol{P}$ of the Riccati equation

$$\begin{bmatrix} \boldsymbol{A}^{\mathrm{T}} & -\boldsymbol{C}^{\mathrm{T}} \\ \boldsymbol{O} & \boldsymbol{O} \end{bmatrix} \boldsymbol{P} + \boldsymbol{P} \begin{bmatrix} \boldsymbol{A} & -\boldsymbol{O} \\ -\boldsymbol{C} & \boldsymbol{O} \end{bmatrix} - \boldsymbol{P} \begin{bmatrix} \boldsymbol{B} \\ \boldsymbol{O} \end{bmatrix} \boldsymbol{R}^{-1} \begin{bmatrix} \boldsymbol{B}^{\mathrm{T}} & \boldsymbol{O} \end{bmatrix} \boldsymbol{P} + \begin{bmatrix} \boldsymbol{Q}_1 & \boldsymbol{O} \\ \boldsymbol{O} & \boldsymbol{Q}_2 \end{bmatrix} = \boldsymbol{O} \tag{4}$$

the feedback gains $\boldsymbol{F}$, $\boldsymbol{G}$, and $\boldsymbol{H}$ are obtained as

$$\boldsymbol{F} = -\boldsymbol{R}^{-1}\boldsymbol{B}^{\mathrm{T}}\boldsymbol{P}_{11} \tag{5}$$

$$\boldsymbol{G} = -\boldsymbol{R}^{-1}\boldsymbol{B}^{\mathrm{T}}\boldsymbol{P}_{12} \tag{6}$$

$$\boldsymbol{H} = \begin{bmatrix} -\boldsymbol{F} + \boldsymbol{G}\boldsymbol{P}_{22}^{-1}\boldsymbol{P}_{12}^{\mathrm{T}} & \boldsymbol{I} \end{bmatrix} \begin{bmatrix} \boldsymbol{A} & \boldsymbol{B} \\ \boldsymbol{C} & \boldsymbol{O} \end{bmatrix}^{-1} \begin{bmatrix} \boldsymbol{O} \\ \boldsymbol{I} \end{bmatrix} \tag{7}$$

Using these feedback gains, the optimum input $\boldsymbol{u}_{opt}$ is given by

$$\boldsymbol{u}_{opt} = \boldsymbol{F}\boldsymbol{x} + \boldsymbol{G}\boldsymbol{w} + \boldsymbol{H}\boldsymbol{r} - \boldsymbol{G}\boldsymbol{P}_{22}^{-1}\boldsymbol{P}_{12}^{\mathrm{T}}\boldsymbol{x}_{\boldsymbol{0}} - \boldsymbol{G}\boldsymbol{w}_{\boldsymbol{0}} \tag{8}$$

where $\boldsymbol{r}$ is the reference input, $\boldsymbol{x}_{\boldsymbol{0}}$ is the initial state, and $\boldsymbol{\omega}_{\boldsymbol{0}}$ is the integral value of state deviation.

4. Control Input for Actuators

The actuator control input with an integral optimum servo is calculated using Eq. (8). Now, the state of the system $\boldsymbol{x}$ and the input $\boldsymbol{u}$ are defined as

$$\boldsymbol{x} = \begin{bmatrix} \theta_b & \dot{\theta}_b & \theta_l & \dot{\theta}_l \end{bmatrix}^{\mathrm{T}} \tag{9}$$

$$\boldsymbol{u} = \begin{bmatrix} u_{Leg} & u_{Rotor} \end{bmatrix}^{\mathrm{T}} \tag{10}$$

where θ_b is the body angle estimated from an IMU, θ_l is the relative angle between the leg and the body, u_{Leg} is the leg input, and u_{Rotor} is the rotor input. The optimum leg input u_{Leg} is distributed to the four actuators that compose two closed links, and all actuator optimum inputs are

$$\begin{aligned} u_{RF} &= -\frac{1}{4}u_{Leg} & u_{RR} &= \frac{1}{4}u_{Leg} \\ u_{LF} &= \frac{1}{4}u_{Leg} & u_{LR} &= -\frac{1}{4}u_{Leg} \end{aligned} \tag{11}$$

u_{RF}, u_{RR}, u_{LF}, and u_{LR} are inputs of the front and rear actuators that compose the left and right closed links. The left and right legs share the optimum input, since yaw rotation is not considered in this model.

5. Attitude Estimation

The coordinate system of the IMU mounted on the robot is indicated by arrows in Fig. 1. The robot is structurally unstable for y-axis rotation since the ankle joint is not fixed. Therefore, it is necessary to estimate the attitude angle around the y-axis to control the attitude of the robot.

In general, attitude angle estimation using an IMU is performed by calculating the gravity direction from the acceleration sensor value. The angle around the y-axis, θ_y, is calculated using Eq. (12) with the accelerations a_x and a_z.

$$\theta_y = \tan^{-1}\left(\frac{a_x}{a_z}\right) \tag{12}$$

Figure 4 shows the estimated attitude angle around the y-axis obtained using Eq. (12). To compare the estimation accuracy of the attitude angle using an IMU, the rotation angle measured using a potentiometer is also plotted in Fig. 4.

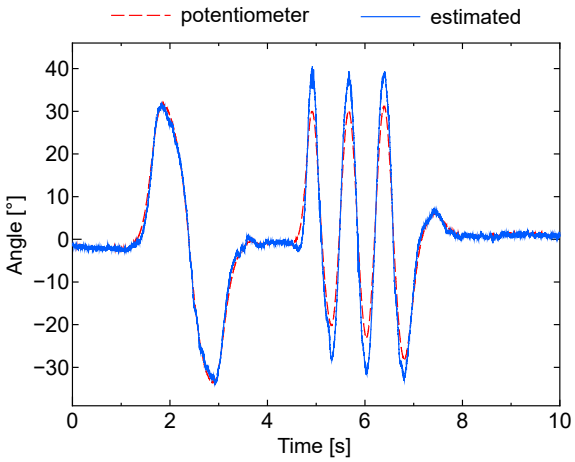

Figure 4: Estimated attitude angle

Here, the estimated angle has an offset caused by the inclination of the sensor mount. It is removed beforehand by subtracting the average of measurements in the stable state.

As a result, the estimated angle using the acceleration sensor has noise and overshoots due to acceleration in accordance with translational motions and vibrations of the robot body. The effects of the noise on the control performance are discussed below.

6. Experimental Results

Attitude stabilization control was conducted in place to confirm the effectiveness of the integral optimum servo controller for the proposed robot model. The weight matrices are defined as

$$\boldsymbol{Q}_1 = \mathrm{diag}\begin{pmatrix} 2\times10^4 & 100 & 1\times10^3 & 1 \end{pmatrix} \tag{13}$$

$$\boldsymbol{Q}_2 = \mathrm{diag}\begin{pmatrix} 1\times10^5 & 1\times10^4 \end{pmatrix} \tag{14}$$

$$\boldsymbol{R} = \mathrm{diag}\begin{pmatrix} 1 & 2 \end{pmatrix} \tag{15}$$

to determine the feedback gains. Input current to actuators is limited to ±3 A by the motor driver. The sampling time of the control is set to 5 ms.

The simulation is also executed by Simscape Multibody in MATLAB/Simulink for comparison to determine the effects of modeling errors.

6.1 Results of attitude control

Figure 5 shows attitude stabilization control results of the developed robot and simulation model. The initial attitude of the actual robot is set at a stable point while supporting the robot with our hands, and in the simulation, $\theta_b = 1°$ and $q_l = 0°$. Both reference inputs of θ_b and θ_l are set to zero. Here, the attitude angle of the actual robot is mechanically limited to ±20° to prevent the robot from falling down.

(a) $t = 0.1$ s **(b)** $t = 0.2$ s **(c)** $t = 0.3$ s **(d)** $t = 0.4$ s **(e)** $t = 0.5$ s **(f)** $t = 0.6$ s **(g)** $t = 0.7$ s

Figure 7: State of attitude stabilization control

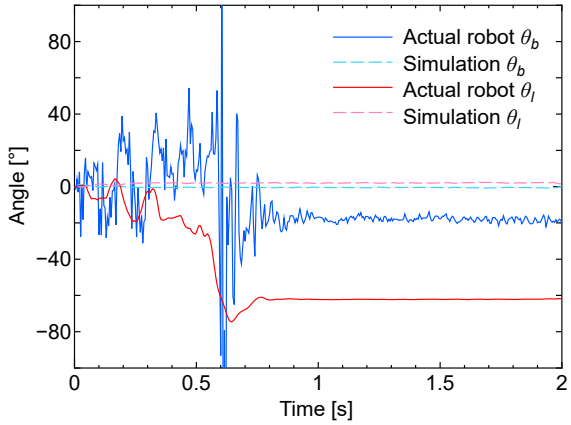

Figure 5: Attitude stabilization control results

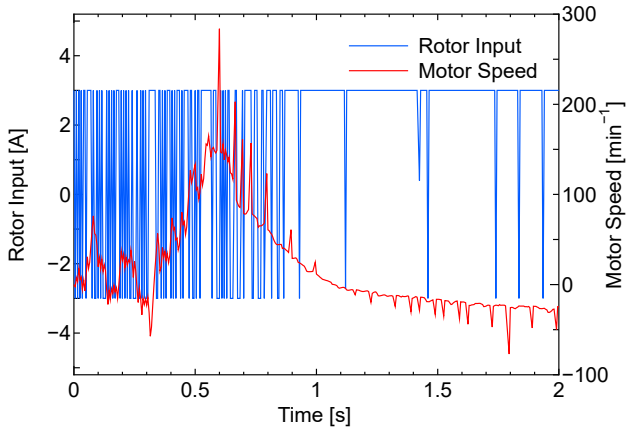

Figure 6: Input and speed of inertial rotor control motor

From the body angle in Fig. 5, it is confirmed that attitude control is successful with no vibration or steady-state deviation from the simulation result. In contrast, the actual robot fell down at around 0.6 s, and then, the attitude of the robot was held at $-20°$ by colliding with support because of the mechanical angle limitation at $\pm 20°$ for safety. Thus, the estimated body angle of more than $\pm 20°$ is considered to originate from the overshoot and momentary impact on the IMU. Moreover, this uncertain attitude angle caused the control input to deviate from the optimal and the actual robot fell down.

Although the relative leg angle of the actual robot in Fig. 5 was controlled to reverse the attitude angle, the attitude stabilization was not achieved. In addition, although the attitude was reversed from 0.6 s to 0.7 s in Fig. 7, the relative leg angle was not reversed in Fig. 5. This is because the rotating shaft was not sufficiently fixed and the leg torque is not reflected in the attitude owing to slip on the shaft.

From the speed of the inertial rotor control motor on the actual robot shown in Fig. 6, it is found that rapid speed change occurred immediately before the robot fell down from 0.46 s to 0.55 s. The inertial rotor generates a reaction force for stabilization by rotating in response to the control input, but the inertial rotor cannot achieve a high rate of acceleration since it has a large moment of inertia. However, the speed of the inertial rotor increased rapidly at about 0.6 s, which we believe was caused by the slipping of the timing belt, and the apparent moment of inertia on the motor shaft decreased. This is also evidenced by the fact that the rotation speed resumes its previous level after the sharp peak. It is considered that the slipping that causes the inability to properly transmit torque is also a major factor in the fall of the robot.

7. Conclusions

In this study, we investigated the attitude control of a biped hopping robot using an inertial rotor in the actual robot. However, the stabilization of the robot attitude was not achieved because of sensor noise and a structural problem of hardware. To realize attitude stabilization, it is necessary to accurately estimate the attitude angle of the robot and strengthen the robot structure to transmit torque reliably.

References

[1] M. Ikeda and N. Suda: Synthesis of optimal servosystems, Transactions of the Society of Instrument and Control Engineers, Vol. 24, No. 1, pp. 40–46, 1988.

[2] H. Suzuki, Y. Yamanaka, T. Kitajima, A. Kuwahara and T. Yasuno: Jumping movement control of biped robot with spring and closed link mechanism, National Convention record I.E.E. Japan, Industry Applications Society, No. 2-S9-7, pp. II-53–II-58, 2021.